processes

MDPI

Article

Multi-Variable Multi-Objective Optimization Algorithm for Optimal Design of PMa-SynRM for Electric Bicycle Traction Motor

Ji-Chang Son [1], Kyung-Pyo Yi [2] and Dong-Kuk Lim [1,*]

[1] Department of Electrical, Electronic and Computer Engineering, University of Ulsan, Ulsan 44610, Korea; wlckd1116@naver.com
[2] Korea Railroad Research Institute, Uiwang 16105, Korea; kpyi82@krri.re.kr
* Correspondence: ldk8745@ulsan.ac.kr; Tel.: +82-52-259-1072

Abstract: In this paper, internal division point genetic algorithm (IDP-GA) was proposed to lessen the computational burden of multi-variable multi-objective optimization problem using finite element analysis such as optimal design of electric bicycles. The IDP-GA could consider various objectives with normalized weighted sum method and could reduce the number of function calls with novel crossover strategy and vector-based pattern search method. The superiority of the proposed algorithm was verified by comparing performances with conventional optimization method at two mathematical test functions. Finally, the applicability of the IDP-GA in practical electric machine design was verified by successfully deriving an improved design of electric bicycle propulsion motor.

Keywords: design optimization; finite element analysis; heuristic algorithms; permanent magnet motors

Citation: Son, J.-C.; Yi, K.-P.; Lim, D.-K. Multi-Variable Multi-Objective Optimization Algorithm for Optimal Design of PMa-SynRM for Electric Bicycle Traction Motor. *Processes* **2021**, *9*, 1901. https://doi.org/10.3390/pr9111901

Academic Editor: Ján Pitel'

Received: 29 September 2021
Accepted: 23 October 2021
Published: 25 October 2021

1. Introduction

Electric bicycles (EBs) are getting more attention in many countries for their convenience, long travelling distance, and environment friendly features [1–3]. In addition, businesses using EBs such as public EB sharing are emerging and EB propulsion motor with low cost and high performance is needed [4].

When designing a motor for EBs, high torque density and improving the riding impression through the reduction of noise and vibration are required [3,5]. Permanent magnet assisted synchronous reluctance motors (PMa-SynRM) have the advantage of high torque density as it utilizes both magnet torque and reluctance torque [6–8]. Also, with the usage of an inexpensive ferrite magnet instead of expensive rare earth magnet, PMa-SynRM is competitive for the manufacturing cost [9,10]. Hence, PMa-SynRM seems to be suitable for the EB propulsion motor.

To relieve the noise and vibration of the motor, various performances such as total harmonic distortion (THD) of back electromotive force (B-EMF), cogging torque, and torque ripple should be considered, and those characteristics can be improved by adjusting the variables related to the structure of the motor [11,12]. Therefore, optimal design of the PMa-SynRM can be defined as a multi-objective, multi-variable (MVMO) problem. Moreover, finite element analysis (FEA) is required for accurate analysis of electric machines [13]. However, the FEA has the disadvantage of huge computational cost, and such a burden becomes worse when the FEA is applied to optimization of the MVMO problems. Therefore, this paper proposes the novel optimization algorithm that can consider many variables and many objective functions simultaneously with a reduced number of function calls.

Many heuristic algorithms were proposed to find the global optima. Specifically, genetic algorithm (GA), which refers to a computational model that simulates the natural selection of Darwin's biological evolution has been widely used [14]. Even though conventional GA guarantees the possibility of finding the global solution, the problem that the

GA requires many populations and iterations which leads to huge computational burden still exists [15].

For the motor design optimization problem, multi-modal optimization algorithm, such as niching GA (NGA), was proposed to find both global and local solutions [12]. However, the NGA can consider only one objective, and has a problem with limited variables as the niche concept is used. Therefore, a novel optimization algorithm that can consider multiple variables and multiple objectives is required.

The internal division point genetic algorithm (IDP-GA) is a novel memetic algorithm modified GA. The IDP-GA has an unusual crossover strategy that is based on the size of objective function values of the parent entities. Novel crossover strategy accelerates convergence speed at the early stage of the algorithm. At the end of the algorithm, a new deterministic method, vector-based pattern search method (VPSM) is used to reduce the duplicated search near the accurate global solution. Moreover, the VPSM enhances the convergence rate of the solution. Furthermore, weighted sum method (WSM) is used to consider various objectives, and likewise for one objective [16]. The proposed algorithm is validated by applying to mathematical test functions and comparing performance with conventional algorithm. Finally, to verify the applicability of actual electric machines, proposed algorithm is applied to optimal design of PMa-SynRM for EBs and successfully derives design with superior performances.

2. Proposed Algorithm

The GA is one of the heuristic algorithms that can successfully converge to a global solution [15,17]. However, the GA has a problem with requiring many function calls to converge to a global solution and cannot consider various objective functions at once. To consider multi-objective, the IDP-GA utilize WSM, which is a method of multiplying weights to each objective and adding together. Also, the number of function calls can be reduced with internal division point concept and VPSM.

2.1. Weighted Sum Method

The WSM is one of the multi-objective methods and can simply reduce several objectives to one objective. Since the units may be different, fitness of each objective can be normalized as

$$f_{i-cal} = (f_i - f_{base-i})/f_{base-i} \tag{1}$$

where f_{base-i} is the reference value, f_i is real value, and f_{i-cal} is normalized value of objective i. The reference values of each objective are determined by analysing the intial model. The fitness calculated by WSM can be expressed as

$$f_{sum} = \sum_{n=1}^{nf} c_n f_{n-cal}, \quad \sum_{n=1}^{nf} c_n = 1 \tag{2}$$

where nf is the number of objectives, c_n is weight assigned to the objective n. For example, when the target motor has high torque ripple and low cogging torque, reducing the torque ripple is more critical, and higher weight is assigned for torque ripple than cogging torque. Accordingly, the designer can perform optimization by giving the desired weight to each objective with the WSM.

2.2. Novel Crossover Strategy- Internal Dividing Point Crossover

Conventional GA converges to global solution by selecting superior entities as parents and generating crossover in the middle of selected two parents. To enhance the convergence speed, the proposed algorithm applies novel crossover strategy named IDP. The IDP literally generates crossover not on the middle point, but on the point divided by objective values of two parents. Figure 1 shows the difference between a conventional approach and IDP. Conventional crossover, which is a blue dot, is generated in the center of two parents.

However, the location of the red dot is determined as the f_{p1} and f_{p2}, which are objective values of parents. The distance is calculated as

$$d_1 = d \times \frac{f_{p2}}{f_{p1} + f_{p2}}, \quad d_2 = d \times \frac{f_{p1}}{f_{p1} + f_{p2}} \tag{3}$$

and then, the position of IDP crossover can be expressed as

$$p(x) = \frac{d_2 x_{p1} + d_1 x_{p2}}{d_1 + d_2} \tag{4}$$

where x_{p1} and x_{p2} are the coordinates of the parents. With the usage of IDP concept, superior crossover can be obtained.

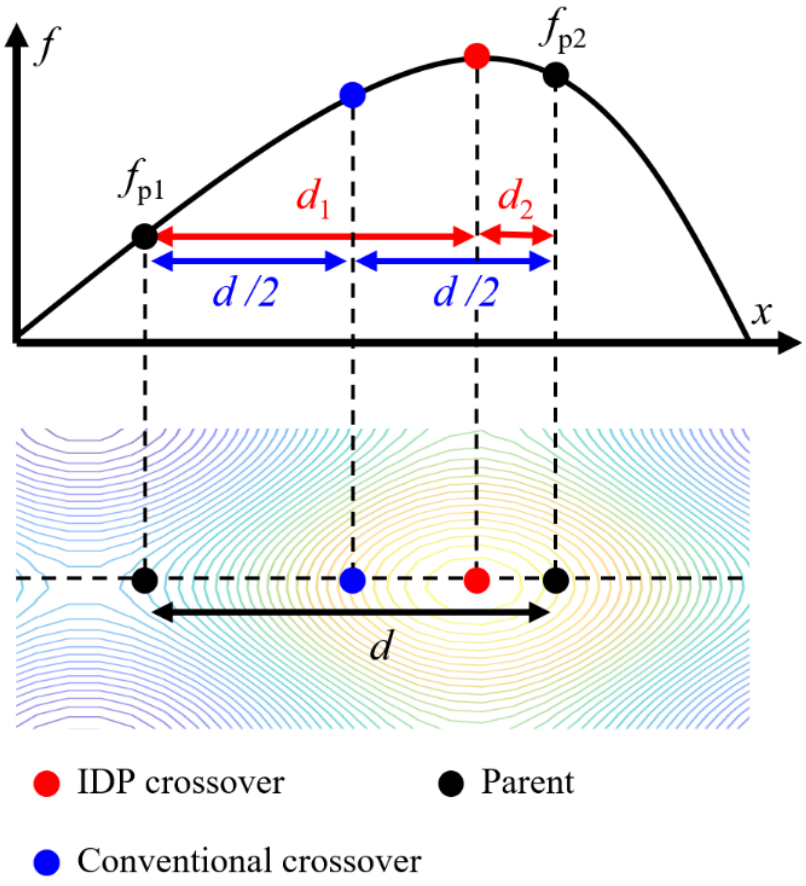

Figure 1. Comparison of conventional crossover and IDP crossover.

2.3. Vector Based Pattern Search Method

At the end of the algorithm, if the populations are regarded as gathered near the global solution, VPSM is executed on the estimated solution to find the actual global solution, preventing unnecessary function calls, and enhancing the convergence characteristic. The criterion of the execution of the VPSM is whether the top 50% fitness group of the population is gathered. The value of 50% was determined through several trials. The VPSM has pattern move and exploration move. On the pattern move step, unit direction vector is determined using objective value of infinitesimal displacement of starting point. Left side of Figure 2 shows an example of calculating direction vector. The number of variables is 2, the starting point is "O", and d is the infinitesimal displacement. Assuming that the

problem region is continuous, with two function calls on the point DX and DY, the values of DX′ and DY′ can be calculated as follows.

$$Z_1' = 2Z - Z_1, \;\; Z_2' = 2Z - Z_2 \tag{5}$$

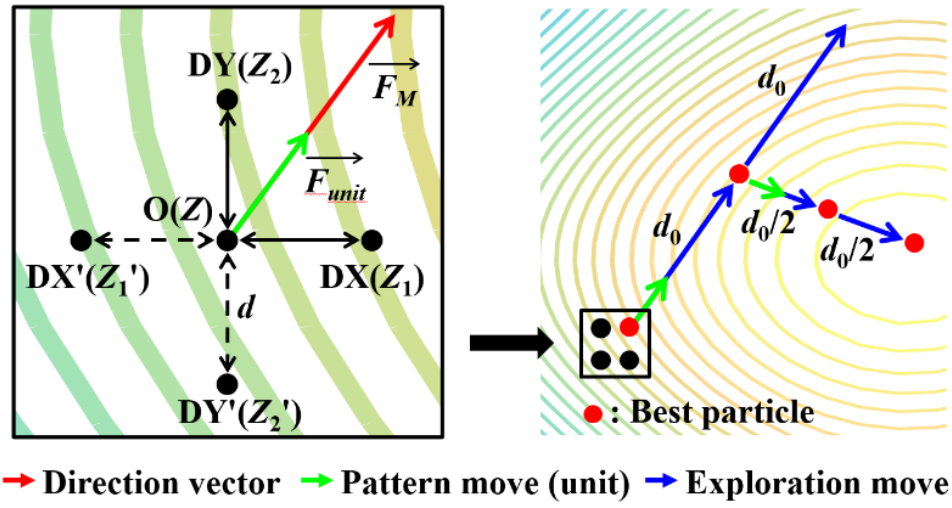

Figure 2. Conceptual schematic of VPSM.

Then, increasing direction of each variable is determined and if DX and DY are points of the increasing direction, the direction vector of each variable can be expressed as follows and marked as red vector line.

$$\vec{F_1} = (Z_1 - Z)\hat{x}, \; \vec{F_2} = (Z_2 - Z)\hat{y}, \; \vec{F_M} = \vec{F_1} + \vec{F_2} \tag{6}$$

Finally, the unit direction vector is calculated as below.

$$\vec{F_{unit}} = \left(\sum_{n=1}^{nf} \vec{F_n}\right) / \left(\left|\sum_{n=1}^{nf} \vec{F_n}\right|\right) \tag{7}$$

Then, the exploration move is performed with preset initial moving distance to determined direction, until the objective value decreases. If the value of next point decreases, pattern move is repeated on the previous point and exploration move with reduced moving distance. As the proposed VPSM adjust the moving direction using the objective values of each variable, the effective search toward the near solution is conducted. Moreover, the number of function calls to converges to the solution can be reduced.

2.4. Flow Chart of the IDP-GA

The flow chart of the proposed algorithm is shown in Figure 3. First, the objective function, parameters, and constraints are defined. Initial solutions are evenly scattered throughout the entire problem region with Latin hypercube sampling method [12,18]. When new entities are added, the total fitness is calculated using Equation (2). In the single objective maximization problem, fitness is proportional to the objective function value. However, for the multi-objective problems, total fitness is calculated as the summation of each objective function value multiplied by assigned weight.

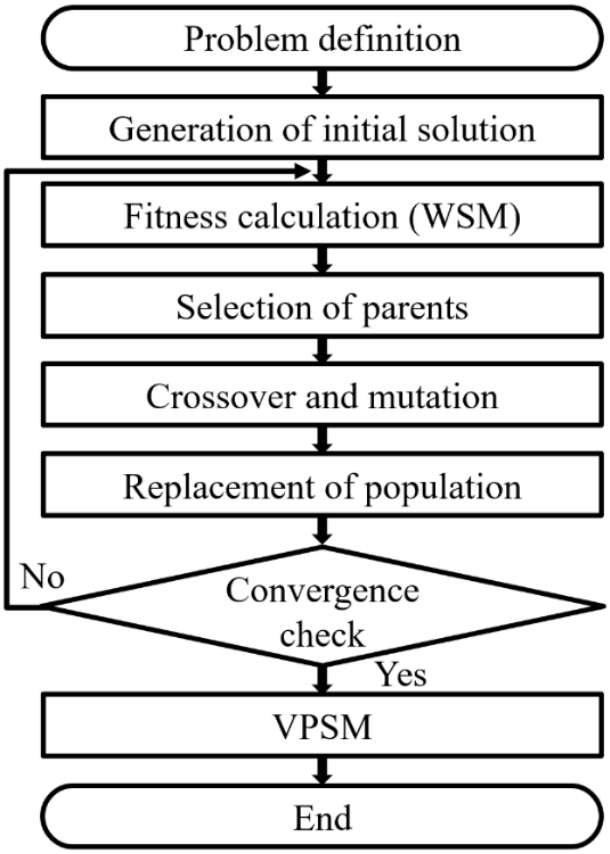

Figure 3. Flow chart of the IDP-GA.

Parents are selected by roulette wheel selection method, and the probability of being selected is proportional to the fitness of each entity. Then, crossover is generated at the IDP of two parents, considering fitness of the parents. Mutants are randomly generated throughout the problem region to prevent the premature convergence to the local solutions. Newly generated crossovers and mutants replace the inferior entities of prior generation. Such loop is repeated until the populations are regarded as gather near the global solution. Finally, VPSM is applied to entity with highest fitness, and direct and rapid convergence to global solution is executed.

3. Performance Validation

To verify the performance of the proposed algorithm, IDP-GA and conventional GA were applied to optimization of two complex mathematical test functions with two and three variables. Test functions are shown in Figure 4 and are defined as

$$f_1(x,y) = \sum_{i=1}^{np_1} \frac{b_i}{1 + \left[(x-x_i)^2 + (y-y_i)^2\right]/a_i} \tag{8}$$

$$f_2(x,y,z) = \sum_{k=1}^{np_2} \frac{10}{\sqrt{(x-x_k)^2 + (y-y_k)^2 + (z-z_k)^2} + c_k} \tag{9}$$

where np_1 and np_2 are the number of solutions, (x_i, y_i) and (x_k, y_k, z_k) are the position of the actual solution. a_i, b_i, and c_k determine the values of the solutions. The number of solutions of test functions 1 and 2 are 11 and 4, respectively. The b_i values are (20, 30, 25, 35, 40, 23, 50, 80, 60, 30, 25) where i = 1~11.

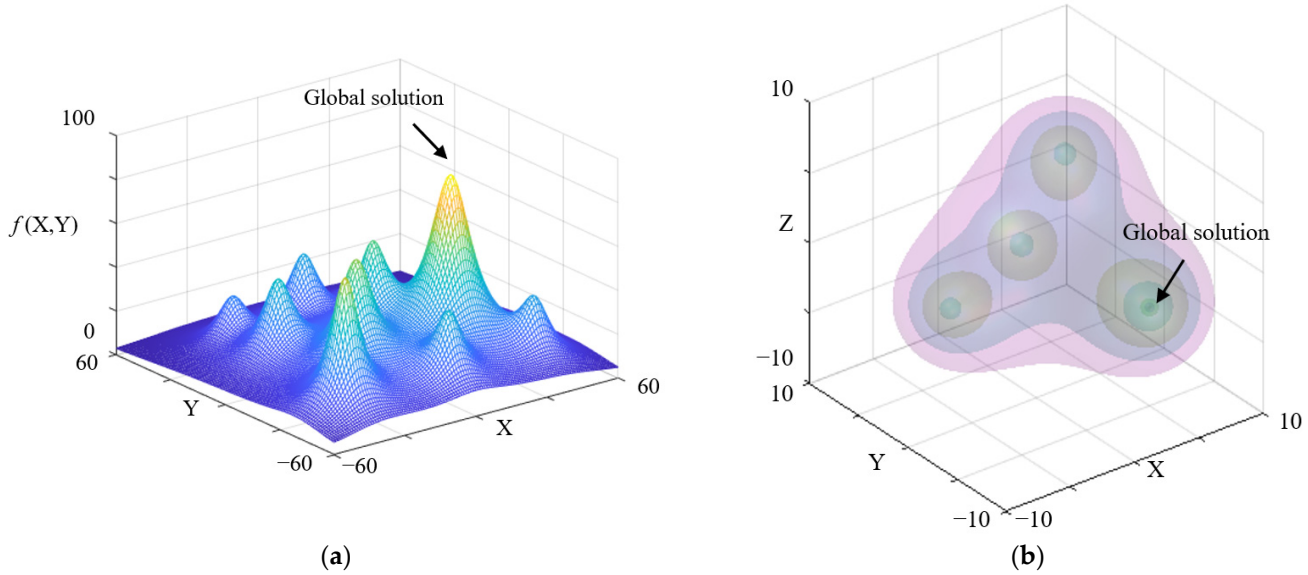

Figure 4. Mathematical test functions (**a**) Test function 1 with 2 variables; (**b**) Test function 2 with 3 variables.

The number of function calls to converge to the global solution and convergence ratio, which is ratio of the found solution to actual solution, are the criteria for evaluating performance. Test was repeated 100 times, and the average of each test result is listed on Table 1. The number of function calls of IDP-GA decreased by 56.27% and 58.21% compared with GA. Specifically, when the number of variable increases, such as in test function 2, the GA has a problem with converging to a local solution rather than a global solution. However, the IDP-GA could converge to an exact global solution within a fewer number of function calls.

Table 1. Performance comparison of conventional GA and IDP-GA.

Test Function 1 [2 Variables]	**Function Call [Average Value]**	**Convergence Ratio [%]**
GA	427.92	98.64
IDP-GA	187.19	99.69
Test Function 2 [3 Variables]	**Function Call [Average Value]**	**Convergence Ratio [%]**
GA	2410.00	75.45
IDP-GA	727.00	92.05

4. Optimal Design of PMa-SynRM for Electric Bicycle Traction Motor

To verify the applicability of the practical electric machine design, the IDP-GA was applied to optimal design of PMa-SynRM for EB propulsion motor. Commercial FEA tool JMAG is used to analyze the load and no-load condition of the target motor [19]. The specifications and requirements of the target motor are tabulated on Table 2. For the purpose of relieving the noise and vibration of the motor, and reducing the pulsation on the torque, cogging torque, and B-EMF waveform, two-stepped skewed rotor structure is applied [20–23].

When designing the motor, various performances should be considered, and the performance varies depending on the shape of the motor [24]. In this paper, to derive the optimal design of the target motor, five variables and three objectives are selected. For design variables, the pole-arc-to-pole-pitch ratios (α_1, α_2), magnet angle (θ), length of the magnet end part (*length*), and slot opening are selected. Design variables and 1/4 periodic

analysis model are shown in Figure 5, and the ranges of each variable are listed on Table 3. The objective function f is calculated as

$$f = f_{thd} \times 0.4 + f_{t\_ripple} \times 0.4 + f_{cogging} \times 0.2 \quad (10)$$

where f_{thd} is THD of line-to-line B-EMF, f_{t_ripple} is torque ripple, and $f_{cogging}$ is percentage of cogging torque to average torque. As the torque ripples, cogging torque and B-EMF THD all have the smaller, better characteristics, and the optimization problem is a minimizataion of f. Optimal design of the target motor was carried out utilizing the proposed IDP-GA, and each function call means execution of the FEA for one design, of which design variables are applied.

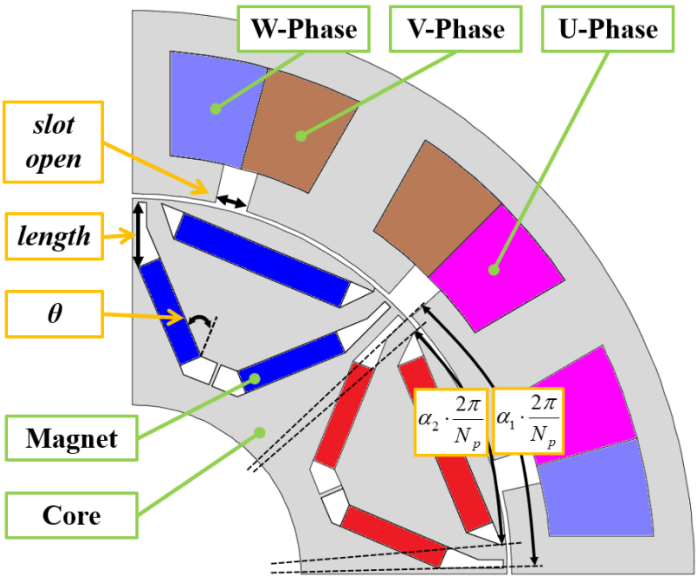

Figure 5. Configuration of the target PMa-SynRM and design variables.

Table 2. Specifications and requirements of the target motor.

Pole/slot	8/12
Stator outer diameter	120 [mm]
Stacking length	20 [mm]
Air gap	0.5 [mm]
Stator and rotor core material	POSCO 35PN230
Permanent magnet material	Ferrite 12G (Br_{min}: 0.44 [T])
Rated output/torque	350 [W]/1.114 [Nm]
Rated/maximum speed	3000/10,000 [RPM]

Table 3. Range of design variables.

Design Variable	Range
α_1	0.92~0.98
α_2	0.65~0.83
θ [°]	40~52
length [mm]	6.0~7.5
slot open [mm]	1~10

The optimization result is tabulated in Table 4 and performances of initial model and optimum model are compared. Torque, cogging torque, and line-to-line B-EMF waveform of initial model and optimum model are shown in Figure 6. For the load analysis of optimum model, the average torque was 8.14% increased, and the torque ripple was 73.43%

reduced compared with initial model. For the no-load analysis, the cogging torque and THD of line-to-line B-EMF was 36.86% and 52.57% improved than initial model. The magnetic flux density contour plot of the optimum model is shown in Figure 7.

Table 4. Optimization result and performance comparison of the initial model and optimum model.

Model	Initial Model	Optimum Model
α_1	0.93	0.96
α_2	0.66	0.81
θ [°]	51.0	45.0
length [mm]	7.4	6.9
slot open [mm]	9.7	3.7
Average torque [Nm]	1.057	1.143
Torque ripple [%]	50.73	13.48
Cogging torque [Nm]	0.0407	0.0257
B-EMF THD [%]	9.34	4.43

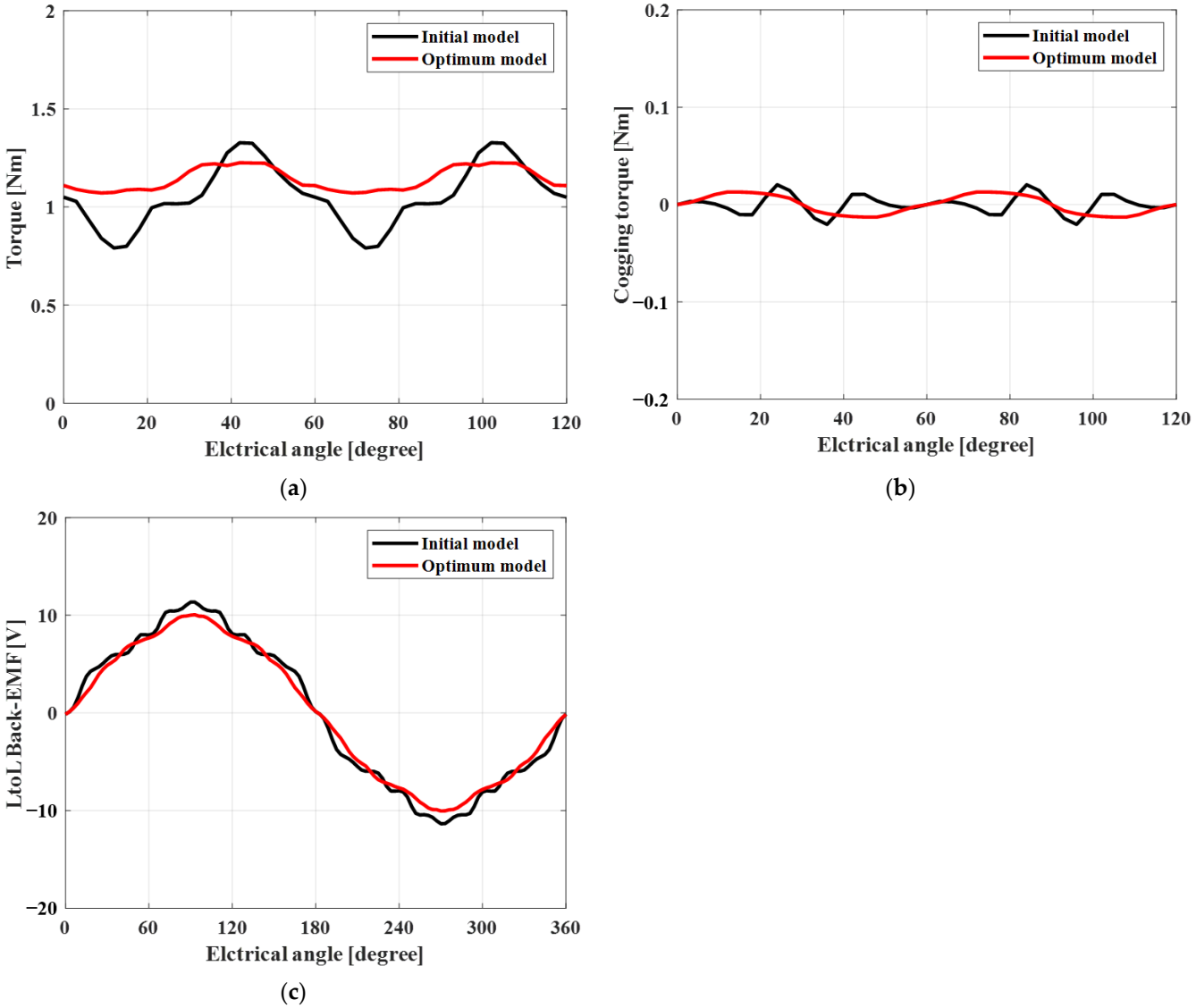

Figure 6. Waveform comparison of the initial model and optimum model (**a**) Torque waveform; (**b**) Cogging torque waveform; (**c**) Line to line B-EMF.

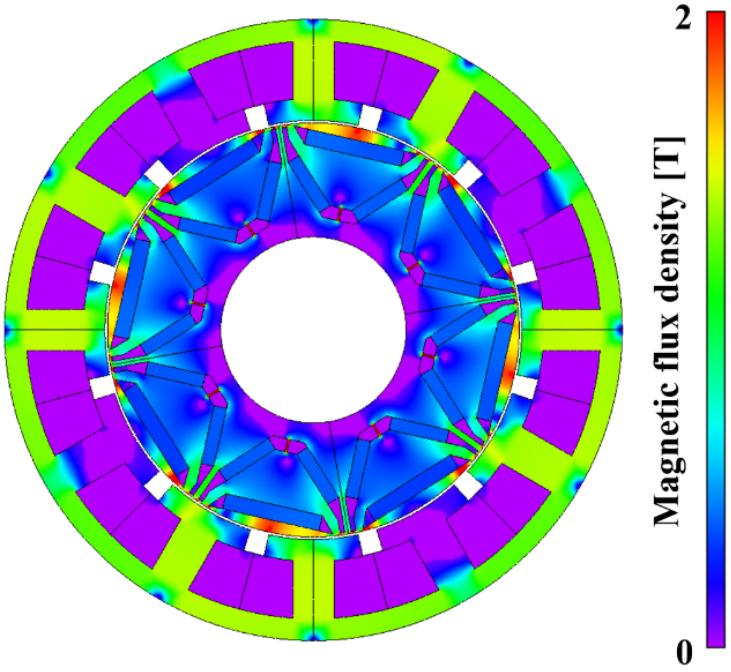

Figure 7. Load condition magnetic flux density contour plot of the optimum model.

To confirm that the optimum model is safe from breakage at rated and maximum rotation speed, mechanical analysis is conducted. The parameters for the mechanical stress analysis are listed on Table 5. Table 6 and Figure 8 shows the Von Mises stress at the rated speed and maximum speed, and the maximum Von Mises stress value was 12.48 MPa and 138.72 MPa, respectively. As the yield stress value of rotor core is 450 MPa, the optimum model is safe from breakage at the maximum rotation speed [25].

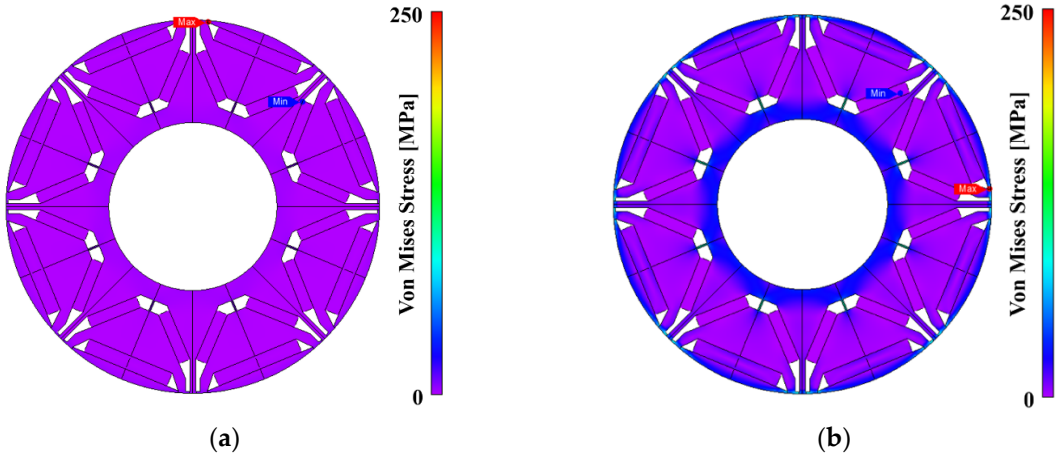

Figure 8. Von Mises stress analysis result of the optimum model (**a**) At rated speed; (**b**) At maximum speed.

Table 5. Parameters for the mechanical stress analysis.

Young's modulus (Core/Ferrite)	210/190 [GPa]
Poisson's ratio (Core/Ferrite)	0.3/0.35
Density (Core/Ferrite)	7850/5100 [kg/m^3]
Rotation speed (Rated/Maximum)	3000/10,000 [RPM]
Yield stress of the core	450 [MPa]

Table 6. Mechanical stress analysis result of the optimum model.

Rotation Speed	Maximum Von Mises Stress Value
3000 [RPM]	12.48 [MPa]
10,000 [RPM]	138.72 [MPa]

5. Conclusions

This paper introduces the IDP-GA to relieve the huge computational burden of the MVMO optimization problem by applying FEA. The IDP-GA accelerated the convergence by applying novel crossover strategy at the early stage of the algorithm. Moreover, convergence rate was enhanced by combining the VPSM. The superiority of the proposed algorithm was validated by applying to mathematical test functions and comparing performances with a conventional algorithm. The applicability of the optimization of actual electric machines was also verified by deriving optimum design with improved performances, when the IDP-GA is applied to the optimal design of PMa-SynRM for EBs. The torque ripple, cogging torque, and B-EMF THD of the optimal model was 73.43%, 36.86% and 52.57% reduced compared to the initial model. The proposed algorithm is expected to be utilized for the MVMO optimization design problem of various types of motors.

Author Contributions: Investigation, J.-C.S.; writing—original draft preparation, J.-C.S.; writing—review and editing, K.-P.Y. and D.-K.L. All authors have read and agreed to the published version of the manuscript.

Funding: This research received no external funding.

Acknowledgments: This research was supported by a grant(21RTRP-B146053-04) from Railroad Technology Research Program (RTRP) funded by Ministry of Land, Infrastructure and Transport of Korean government.

Conflicts of Interest: The authors declare no conflict of interest.

References

1. Li, Y.; Hu, J.; Chen, F.; Liu, Z.Y.; He, Z. A New-Variable-Coil-Structure-Based IPT System with Load-Independent Constant Output Current or Voltage for Charging Electric Bicycles. *IEEE Trans. Power Electron.* **2018**, *33*, 8226–8230. [CrossRef]
2. Hsu, R.C.; Liu, C.; Chan, D. A Reinforcement-Learning-Based Assisted Power Management with QoR Provisioning for Human–Electric Hybrid Bicycle. *IEEE Trans. Ind. Electron.* **2012**, *59*, 3350–3359. [CrossRef]
3. Lim, D.; Cho, Y.; Ro, J.; Jung, S.; Jung, H. Optimal Design of an Axial Flux Permanent Magnet Synchronous Motor for the Electric Bicycle. *IEEE Trans. Magn.* **2016**, *52*, 8201204. [CrossRef]
4. Wang, L.; Li, C.; Chen, M.Z.Q.; Wang, Q.; Tao, F. Connectivity-Based Accessibility for Public Bicycle Sharing Systems. *IEEE Trans. Autom. Sci. Eng.* **2018**, *15*, 1521–1532. [CrossRef]
5. Lin, J.; Schofield, N.; Emadi, A. External-Rotor 6-10 Switched Reluctance Motor for an Electric Bicycle. *IEEE Trans. Transp. Electrif.* **2015**, *1*, 348–356. [CrossRef]
6. Xu, M.; Liu, G.; Chen, Q.; Ji, J.; Zhao, W. Torque Calculation of Stator Modular PMa-SynRM with Asymmetric Design for Electric Vehicles. *IEEE Trans. Transp. Electrif.* **2021**, *7*, 202–213. [CrossRef]
7. Joo, K.; Kim, I.; Lee, J.; Go, S. Robust Speed Sensorless Control to Estimated Error for PMa-SynRM. *IEEE Trans. Magn.* **2017**, *53*, 8102604. [CrossRef]
8. Jung, D.-H.; Kwak, Y.; Lee, J.; Jin, C. Study on the Optimal Design of PMa-SynRM Loading Ratio for Achievement of Ultrapremium Efficiency. *IEEE Trans. Magn.* **2017**, *53*, 8001904. [CrossRef]
9. Amin, M.; Aziz, G.A.A. Hybrid Adopted Materials in Permanent Magnet-Assisted Synchronous Reluctance Motor with Rotating Losses Computation. *IEEE Trans. Magn.* **2019**, *55*, 8103305. [CrossRef]
10. Kong, Y.; Lin, M.; Yin, M.; Hao, L. Rotor Structure on Reducing Demagnetization of Magnet and Torque Ripple in a PMa-synRM With Ferrite Permanent Magnet. *IEEE Trans. Magn.* **2018**, *54*, 8108705. [CrossRef]
11. Son, J.-C.; Kang, Y.-R.; Lim, D.-K. Optimal Design of IPMSM for FCEV Using Novel Immune Algorithm Combined with Steepest Descent Method. *Energies* **2020**, *13*, 3395. [CrossRef]
12. Kang, Y.; Son, J.; Lim, D. Optimal Design of IPMSM for Fuel Cell Electric Vehicles Using Autotuning Elliptical Niching Genetic Algorithm. *IEEE Access* **2020**, *8*, 117405–117412. [CrossRef]
13. Son, J.-C.; Ahn, J.-M.; Lim, J.; Lim, D.-K. Optimal Design of PMa-SynRM for Electric Vehicles Exploiting Adaptive-Sampling Kriging Algorithm. *IEEE Access* **2021**, *9*, 41174–41183. [CrossRef]

14. Jiacheng, L.; Lei, L. A Hybrid Genetic Algorithm Based on Information Entropy and Game Theory. *IEEE Access* **2020**, *8*, 36602–36611. [CrossRef]
15. Lee, K.; Oh, H.; Jung, S.; Chung, Y. Moving Least Square-Based Hybrid Genetic Algorithm for Optimal Design of *W*-Band Dual-Reflector Antenna. *IEEE Trans. Magn.* **2019**, *55*, 9400404. [CrossRef]
16. Ryu, N.; Lim, S.; Min, S.; Izui, K.; Nishiwaki, S. Multi-Objective Optimization of Magnetic Actuator Design Using Adaptive Weight Determination Scheme. *IEEE Trans. Magn.* **2017**, *53*, 7205104. [CrossRef]
17. Choi, K.; Jang, D.; Kang, S.; Lee, J.; Chung, T.; Kim, H. Hybrid Algorithm Combing Genetic Algorithm with Evolution Strategy for Antenna Design. *IEEE Trans. Magn.* **2016**, *52*, 7209004. [CrossRef]
18. Davey, K.R. Latin Hypercube Sampling and Pattern Search in Magnetic Field Optimization Problems. *IEEE Trans. Magn.* **2008**, *44*, 974–977. [CrossRef]
19. JMAG-Designer. Available online: https://www.jmag-international.com/products/jmag-designer/ (accessed on 28 September 2021).
20. Torregrossa, D.; Peyraut, F.; Cirrincione, M.; Espanet, C.; Cassat, A.; Miraoui, A. A New Passive Methodology for Reducing the Noise in Electrical Machines: Impact of Some Parameters on the Modal Analysis. *IEEE Trans. Ind. Appl.* **2010**, *46*, 1899–1907. [CrossRef]
21. Kawase, Y.; Yamaguchi, T.; Tu, Z.; Toida, N.; Minoshima, N.; Hashimoto, K. Effects of Skew Angle of Rotor in Squirrel-Cage Induction Motor on Torque and Loss Characteristics. *IEEE Trans. Magn.* **2009**, *45*, 1700–1703. [CrossRef]
22. Lazari, P.; Wang, J.; Sen, B. 3-D Effects of Rotor Step-Skews in Permanent Magnet-Assisted Synchronous Reluctance Machines. *IEEE Trans. Magn.* **2015**, *51*, 8112704. [CrossRef]
23. Bao, X.; Fang, J.; Di, C.; Xu, S. A Novel Computational Method of Skewing Leakage Reactance for a Doubly Skewed Rotor Induction Motor. *IEEE Trans. Energy Convers.* **2018**, *33*, 2174–2182. [CrossRef]
24. Lim, D.; Woo, D.; Yeo, H.; Jung, S.; Ro, J.; Jung, H. A Novel Surrogate-Assisted Multi-Objective Optimization Algorithm for an Electromagnetic Machine Design. *IEEE Trans. Magn.* **2015**, *51*, 8200804. [CrossRef]
25. Ahn, J.-M.; Baek, M.-K.; Park, S.-H.; Lim, D.-K. Optimal Design of IPMSM for EV Using Subdivided Kriging Multi-Objective Optimization. *Processes* **2021**, *9*, 1490. [CrossRef]